

## 58. $\tau$ Branching Fractions

Revised May 2019 by Sw. Banerjee (Louisville U.) and A. Lusiani (SNS, Pisa; INFN, Pisa).

### 58.1 $\tau$ Branching Fractions

The  $\tau$  Listings contains 244 entries that correspond to either a  $\tau$  partial decay fraction into a specific decay mode (branching fraction) or a ratio of two  $\tau$  partial decay fractions (branching ratio). Experimental information provides values for 147 of these quantities, upper limits for 61 branching fractions to Lepton Family number, Lepton number, or Baryon number violating modes, and 36 additional upper limits for other modes. A total of 170 measurements of  $\tau$  branching fraction and branching ratio measurements is used for a global fit that determines 129 quantities.

### 58.2 The constrained fit to $\tau$ branching fractions

The  $\tau$  branching fractions fit uses the reported values, uncertainties and statistical correlations of the  $\tau$  branching fractions and branching ratios measurements. Asymmetric uncertainties are symmetrized as  $\sigma_{\text{symm}}^2 = (\sigma_+^2 + \sigma_-^2)/2$ . Additionally, the most precise experimental inputs are treated according to how they depend on external parameters on the basis of their documentation [1]. The  $\tau$  measurements may depend on parameters such as the  $\tau$  pair production cross-section in  $e^+e^-$  annihilations at the  $\Upsilon(4S)$  peak. In some cases, measurements reported in different papers by the same collaboration may depend on common parameters like the estimate of the integrated luminosity or of particle identification efficiencies. For all the significant detected dependencies, the  $\tau$  measurements and their uncertainties are updated to account for the updated values of the external parameters. The dependencies on common systematic effects are also determined in size and sign, and all the common systematic dependencies of different measurements are used together with the published statistical and systematic uncertainties and correlations in order to compute a single all-inclusive variance and covariance matrix of the experimental inputs of the fit.

The fit procedure parameters correspond to  $\tau$  quantities that are fit to the experimental measurements while respecting relations described by a series of constraint equations. All the experimental inputs and all the constraint equations are reported in the  $\tau$  Listings section that follows this review. With respect to the 2016, 2017 and 2018 editions, the fit uses one more experimental measurement, published by the BaBar collaboration in 2018, on  $\mathcal{B}(\tau \rightarrow K^- K^0 \nu_\tau)$  [2]. If only a few measurements are correlated, the correlation coefficients are listed in the footnote for each measurement (see for example  $\Gamma(\text{particle}^- \geq 0 \text{ neutrals} \geq 0 K^0 \nu_\tau) / \Gamma_{\text{total}}$  (“1-prong”). If a large number of measurements are correlated, then the full correlation matrix is listed in the footnote to the measurement that first appears in the  $\tau$  Listings. Footnotes to the other measurements refer to the first one. For example, the large correlation matrices for the branching fraction or ratio measurements contained in Refs. [3] [4] are listed in Footnotes to the  $\Gamma(e^- \bar{\nu}_e \nu_\tau) / \Gamma_{\text{total}}$  and  $\Gamma(h^- \nu_\tau) / \Gamma_{\text{total}}$  measurements respectively. The constraints between the  $\tau$  branching fractions and ratios include coefficients that correspond to physical quantities, like for instance the branching fractions of the  $\eta$  and  $\omega$  mesons. All quantities are taken from the 2018 edition of the Review of Particle Physics. Their uncertainties are neglected in the fit.

We obtain the branching fraction of  $\tau \rightarrow a_1^- (\rightarrow \pi^- \gamma) \nu_\tau$  using the ALEPH estimate for  $\mathcal{B}(a_1^- \rightarrow \pi^- \gamma)$  [3], which uses the measurement of  $\Gamma(a_1^- \rightarrow \pi^- \gamma)$  [5]. In the fit, we assume that  $\mathcal{B}(\tau^- \rightarrow a_1^- \nu_\tau)$  is equal to  $\mathcal{B}(\tau^- \rightarrow \pi^- \pi^- \pi^+ \nu_\tau)$  (ex.  $K^0, \omega$ ) +  $\mathcal{B}(\tau^- \rightarrow \pi^- 2\pi^0 \nu_\tau)$  (ex.  $K^0$ ), neglecting the observed but negligible branching fractions to other modes, including  $\mathcal{B}(a_1^- \rightarrow \pi^- \gamma)$ .

In some cases, constraints describe approximate relations that nevertheless hold within the present experimental precision. For instance, the constraint  $\mathcal{B}(\tau \rightarrow K^- K^- K^+ \nu_\tau) = \mathcal{B}(\tau \rightarrow K^- \phi \nu_\tau) \times \mathcal{B}(\phi \rightarrow K^+ K^-)$  is justified within the current experimental evidence.

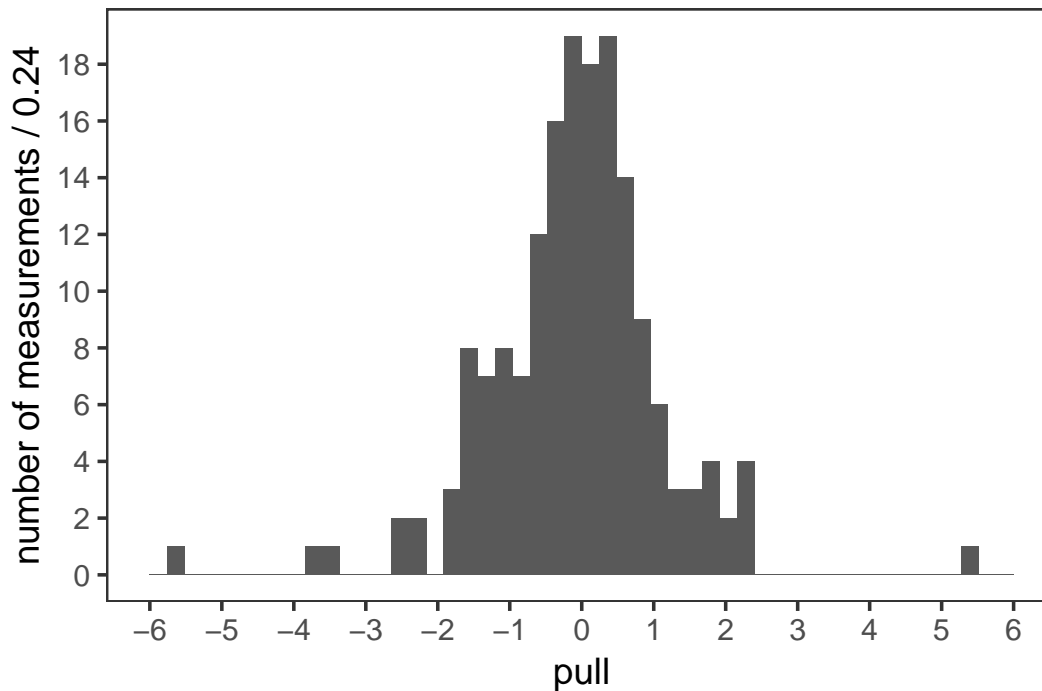


**Figure 58.1:** Pulls of individual measurements against the respective fitted quantity. No scale factor is used.

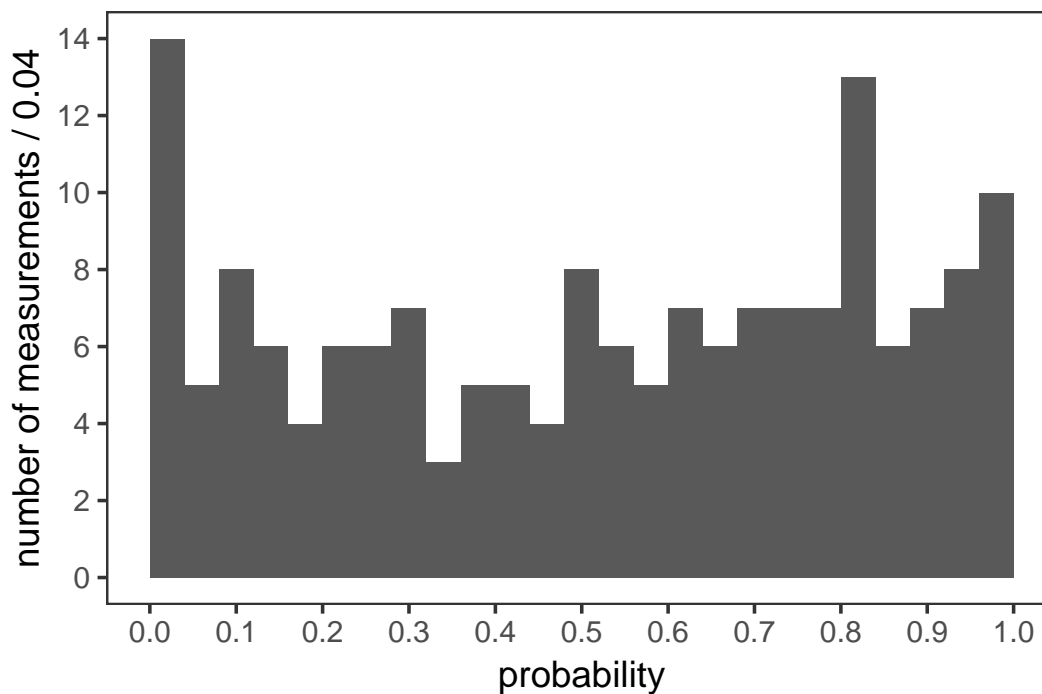


**Figure 58.2:** Probability of individual measurement pulls against the respective fitted quantity. No scale factor is used.

In the fit, scale factors are applied to the published uncertainties of measurements only if significant inconsistency between different measurements remain after accounting for all relevant

uncertainties and correlations. After examining the data and the fit pulls, it has been decided to apply just one scale factor of 5.4 on the measurements of  $\mathcal{B}(\tau \rightarrow K^- K^- K^+ \nu_\tau)$ . The scale factor has been computed and applied according to the standard PDG procedure. Without the scale factor applied, the  $\chi^2$  probability of the fit is about 2%. On a per-measurement basis, the pull distribution in figure 58.1 indicates that just a few measurements have more than  $3\sigma$  pulls. (The uncertainties to obtain the pulls are computed using the measurements variance matrix and the variance matrix of the result, accounting for the fact that the variance matrix of the result is obtained from the measurement variance with the fit.) The pull probability distribution in figure 58.2 is reasonably flat. With many measurements some entries on the tails of the normal distribution must be expected. There are 170 pulls, one per measurement. They are partially correlated, and the effective number of independent pulls is equal to the number of degrees of freedom of the fit, 125. Only the  $\tau \rightarrow K^- K^- K^+ \nu_\tau$  decay mode has a pull that is inconsistent at the level of more than  $3\sigma$  even if considered as the largest pull in a set of 125. This confirms the choice of adopting just that one scale factor.

After scaling the error, the constrained fit has a  $\chi^2$  of 135 for 125 degrees of freedom, corresponding to a  $\chi^2$  probability of 26%. We use 170 measurements and 84 constraints on the branching fractions and ratios to determine 129 quantities, consisting of 112 branching fractions and 17 branching ratios. A total of 85 quantities have at least one measurement in the fit. The constraints include the unitarity constraint on the sum of all the exclusive  $\tau$  decay modes,  $\mathcal{B}_{\text{all}} = 1$ . If the unitarity constraint is released, the fit result for  $\mathcal{B}_{\text{all}}$  is consistent with unitarity with  $1 - \mathcal{B}_{\text{all}} = (0.00 \pm 0.10)\%$ .

For the convenience of summarizing the fit results, we list in the following the values and uncertainties for a set of 46 “basis” decay modes, from which all remaining branching fractions and ratios can be obtained using the constraints. The basis decay modes are not intended to sum up to 1. Since some basis quantities represent multiple branching fractions that are related by constraint equations, they are properly weighted and the unitarity constraint corresponds to a linear combination whose coefficients are listed in the following. The correlation matrix between the basis modes is reported in the  $\tau$  Listings.

decay mode	fit result (%)	coefficient
$\mu^- \bar{\nu}_\mu \nu_\tau$	$17.3937 \pm 0.0384$	1.0000
$e^- \bar{\nu}_e \nu_\tau$	$17.8175 \pm 0.0399$	1.0000
$\pi^- \nu_\tau$	$10.8164 \pm 0.0512$	1.0000
$K^- \nu_\tau$	$0.6964 \pm 0.0096$	1.0000
$\pi^- \pi^0 \nu_\tau$	$25.4941 \pm 0.0893$	1.0000
$K^- \pi^0 \nu_\tau$	$0.4328 \pm 0.0148$	1.0000
$\pi^- 2\pi^0 \nu_\tau$ (ex. $K^0$ )	$9.2595 \pm 0.0964$	1.0021
$K^- 2\pi^0 \nu_\tau$ (ex. $K^0$ )	$0.0647 \pm 0.0218$	1.0000
$\pi^- 3\pi^0 \nu_\tau$ (ex. $K^0$ )	$1.0429 \pm 0.0707$	1.0000
$K^- 3\pi^0 \nu_\tau$ (ex. $K^0, \eta$ )	$0.0478 \pm 0.0212$	1.0000
$h^- 4\pi^0 \nu_\tau$ (ex. $K^0, \eta$ )	$0.1118 \pm 0.0391$	1.0000
$\pi^- \bar{K}^0 \nu_\tau$	$0.8384 \pm 0.0138$	1.0000

decay mode	fit result (%)	coefficient
$K^- K^0 \nu_\tau$	$0.1486 \pm 0.0034$	1.0000
$\pi^- \bar{K}^0 \pi^0 \nu_\tau$	$0.3817 \pm 0.0129$	1.0000
$K^- \pi^0 K^0 \nu_\tau$	$0.1500 \pm 0.0070$	1.0000
$\pi^- \bar{K}^0 2\pi^0 \nu_\tau$ (ex. $K^0$ )	$0.0263 \pm 0.0226$	1.0000
$\pi^- K_S^0 K_S^0 \nu_\tau$	$0.0235 \pm 0.0006$	2.0000
$\pi^- K_S^0 K_L^0 \nu_\tau$	$0.1081 \pm 0.0241$	1.0000
$\pi^- \pi^0 K_S^0 K_S^0 \nu_\tau$	$0.0018 \pm 0.0002$	2.0000
$\pi^- \pi^0 K_S^0 K_L^0 \nu_\tau$	$0.0325 \pm 0.0119$	1.0000
$\bar{K}^0 h^- h^- h^+ \nu_\tau$	$0.0247 \pm 0.0199$	1.0000
$\pi^- \pi^- \pi^+ \nu_\tau$ (ex. $K^0, \omega$ )	$8.9868 \pm 0.0513$	1.0021
$\pi^- \pi^- \pi^+ \pi^0 \nu_\tau$ (ex. $K^0, \omega$ )	$2.7404 \pm 0.0710$	1.0000
$h^- h^- h^+ 2\pi^0 \nu_\tau$ (ex. $K^0, \omega, \eta$ )	$0.0981 \pm 0.0356$	1.0000
$\pi^- K^- K^+ \nu_\tau$	$0.1435 \pm 0.0027$	1.0000
$\pi^- K^- K^+ \pi^0 \nu_\tau$	$0.0061 \pm 0.0018$	1.0000
$\pi^- \pi^0 \eta \nu_\tau$	$0.1389 \pm 0.0072$	1.0000
$K^- \eta \nu_\tau$	$0.0155 \pm 0.0008$	1.0000
$K^- \pi^0 \eta \nu_\tau$	$0.0048 \pm 0.0012$	1.0000
$\pi^- \bar{K}^0 \eta \nu_\tau$	$0.0094 \pm 0.0015$	1.0000
$\pi^- \pi^+ \pi^- \eta \nu_\tau$ (ex. $K^0$ )	$0.0220 \pm 0.0013$	1.0000
$K^- \omega \nu_\tau$	$0.0410 \pm 0.0092$	1.0000
$h^- \pi^0 \omega \nu_\tau$	$0.4085 \pm 0.0419$	1.0000
$K^- \phi \nu_\tau$	$0.0044 \pm 0.0016$	0.8320
$\pi^- \omega \nu_\tau$	$1.9494 \pm 0.0645$	1.0000
$K^- \pi^- \pi^+ \nu_\tau$ (ex. $K^0, \omega$ )	$0.2927 \pm 0.0068$	1.0000
$K^- \pi^- \pi^+ \pi^0 \nu_\tau$ (ex. $K^0, \omega, \eta$ )	$0.0394 \pm 0.0142$	1.0000
$\pi^- 2\pi^0 \omega \nu_\tau$ (ex. $K^0$ )	$0.0072 \pm 0.0016$	1.0000
$2\pi^- \pi^+ 3\pi^0 \nu_\tau$ (ex. $K^0, \eta, \omega, f_1$ )	$0.0014 \pm 0.0027$	1.0000
$3\pi^- 2\pi^+ \nu_\tau$ (ex. $K^0, \omega, f_1$ )	$0.0775 \pm 0.0030$	1.0000
$K^- 2\pi^- 2\pi^+ \nu_\tau$ (ex. $K^0$ )	$0.0001 \pm 0.0001$	1.0000
$2\pi^- \pi^+ \omega \nu_\tau$ (ex. $K^0$ )	$0.0084 \pm 0.0006$	1.0000
$3\pi^- 2\pi^+ \pi^0 \nu_\tau$ (ex. $K^0, \eta, \omega, f_1$ )	$0.0038 \pm 0.0009$	1.0000
$K^- 2\pi^- 2\pi^+ \pi^0 \nu_\tau$ (ex. $K^0$ )	$0.0001 \pm 0.0001$	1.0000
$\pi^- f_1 \nu_\tau$ ( $f_1 \rightarrow 2\pi^- 2\pi^+$ )	$0.0052 \pm 0.0004$	1.0000
$\pi^- 2\pi^0 \eta \nu_\tau$	$0.0195 \pm 0.0038$	1.0000

In defining the fit constraints and in selecting the modes that sum up to one we made some assumptions and choices. We assume that some channels, like  $\tau^- \rightarrow \pi^- K^+ \pi^- \geq 0\pi^0 \nu_\tau$  and  $\tau^- \rightarrow \pi^+ K^- K^- \geq 0\pi^0 \nu_\tau$ , have negligible branching fractions as expected from the Standard Model, even if the experimental limits for these branching fractions are not very stringent. The 95% confidence level upper limits are  $\mathcal{B}(\tau^- \rightarrow \pi^- K^+ \pi^- \geq 0\pi^0 \nu_\tau) < 0.25\%$  and  $\mathcal{B}(\tau^- \rightarrow \pi^+ K^- K^- \geq 0\pi^0 \nu_\tau) < 0.09\%$ , values not so different from measured branching fractions for allowed 3-prong modes containing charged kaons. For decays to final states containing one neutral kaon we assume that the branching fraction with the  $K_L^0$  are the same as the corresponding one with a  $K_S^0$ . On decays with two neutral kaons we assume that the branching fractions with  $K_L^0 K_L^0$  are the same as the ones with  $K_S^0 K_S^0$ .

### 58.3 BaBar and Belle measure on average lower branching fractions and ratios.

We compare the BaBar and Belle measurements with the results of a fit where all their measurements have been excluded. We find that that BaBar and Belle measure on average lower  $\tau$  branching fractions and ratios than the other experiments. Figures 58.3 and 58.4 show histograms of the 28 normalized differences between the  $B$ -factory measurements and the respective non- $B$ -factory fit results. The normalization is the uncertainty on the difference. The average normalized difference between the two sets of measurements is  $-0.8\sigma$  ( $-0.7\sigma$  for the 16 Belle measurements and  $-0.8\sigma$  for the 12 BaBar measurements).

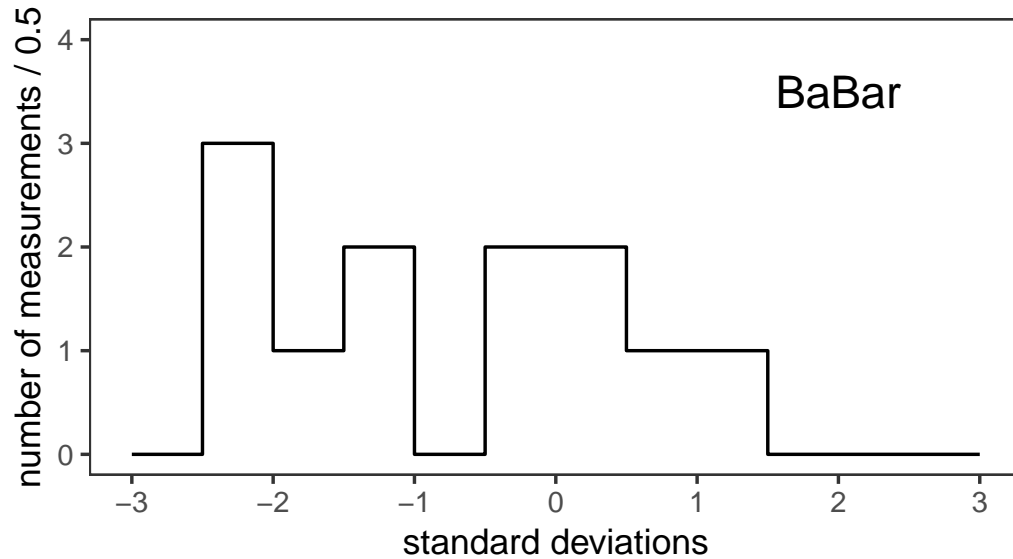


**Figure 58.3:** Distribution of the normalized difference between 12 measurements of branching fractions and ratios published by the BaBar collaboration and the respective averages computed using only non- $B$ -factory measurements.

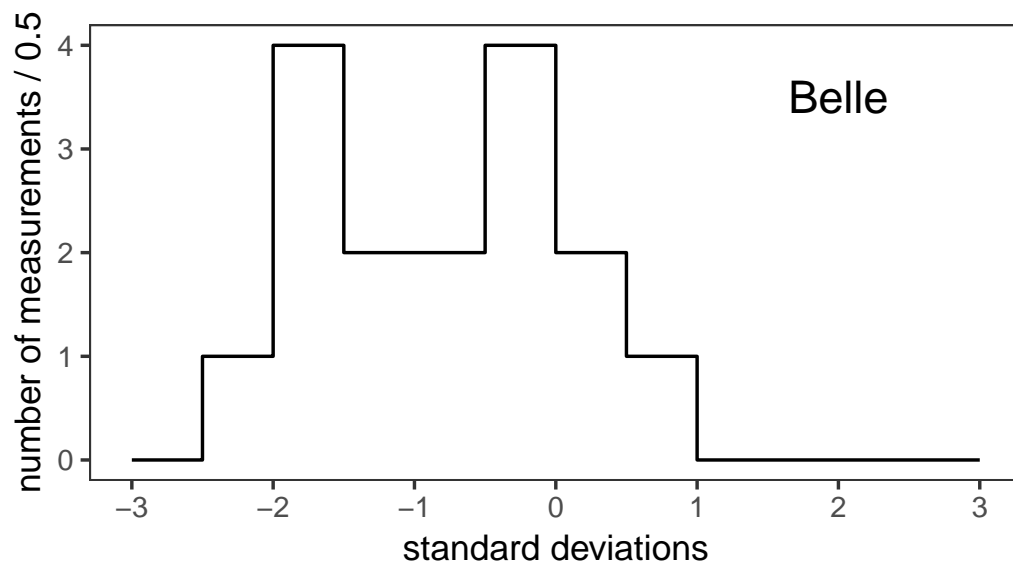


**Figure 58.4:** Distribution of the normalized difference between 16 measurements of branching fractions and ratios published by the Belle collaboration and the respective averages computed using only non- $B$ -factory measurements.

### 58.4 Overconsistency of Leptonic Branching Fraction Measurements.

As observed in the previous editions of this review, measurements of the leptonic branching fractions are more consistent with each other than expected from the quoted errors on the individual measurements. The  $\chi^2$  is 0.34 for  $\mathcal{B}_e$  and 0.08 for  $\mathcal{B}_\mu$ . Assuming normal errors, the probability of a smaller  $\chi^2$  is 1.3% for  $\mathcal{B}_e$  and 0.08% for  $\mathcal{B}_\mu$ .

### 58.5 Technical implementation of the fit

The fit computes a set of quantities denoted with  $q_i$  by minimizing a  $\chi^2$  while respecting a series of equality constraints on the  $q_i$ . The  $\chi^2$  is computed using the measurements  $m_i$  and their covariance matrix  $E_{ij}$  as  $\chi^2 = (m_i - A_{ik}q_k)^t E_{ij}^{-1} (m_j - A_{jl}q_l)$ , where the model matrix  $A_{ij}$  is used to get the vector of the predicted measurements  $m'_i$  from the vector of the fit parameters  $q_j$  as  $m'_i = A_{ij}q_j$ . In this particular implementation the measurements are grouped by the quantity that they measure, and all quantities with at least one measurement correspond to a fit parameter. Therefore, the matrix  $A_{ij}$  has one row per measurement  $m_i$  and one column per fitted quantity  $q_j$ , with unity coefficients for the rows and column that identify a measurement  $m_i$  of the quantity  $q_j$ , respectively. The constraints are equations involving the fit parameters. The fit does not impose limitations on the functional form of the constraints. In summary, the fit requires:

$$\min [\chi^2(q_k)] = \min [(m_i - A_{ik}q_k)^t E_{ij}^{-1} (m_j - A_{jl}q_l)] , \quad (58.1)$$

$$\text{subjected to } f_r(q_s) - c_r = 0 , \quad (58.2)$$

where the left term of Eq. 58.2 defines the constraint expressions. Using the method of Lagrange multipliers, a set of equations is obtained by taking the derivatives with respect to the fitted quantities  $q_k$  and the Lagrange multipliers  $\lambda_r$  of the sum of the  $\chi^2$  and the constraint expressions multiplied by the Lagrange multipliers  $\lambda_r$ , one for each constraint:

$$\begin{aligned} \min [(A_{ik}q_k - m_i)^t E_{ij}^{-1} (A_{jl}q_l - m_j) + 2\lambda_r (f_r(q_s) - c_r)] &= \\ &= \min [\tilde{\chi}^2(q_k, \lambda_r)] , \\ (\partial/\partial q_k, \partial/\partial \lambda_r) [\tilde{\chi}^2(q_k, \lambda_r)] &= 0 . \end{aligned} \quad (58.3)$$

Eq. 58.3 defines a set of equations for the vector of the unknowns  $(q_k, \lambda_r)$ , some of which may be non-linear, in case of non-linear constraints. An iterative minimization procedure approximates at each step the non-linear constraint expressions by their first order Taylor expansion around the current values of the fitted quantities,  $\bar{q}_s$ :

$$f_r(q_s) - c_r = f_r(\bar{q}_s) + \left. \frac{\partial f_r(q_s)}{\partial q_s} \right|_{\bar{q}_s} (q_s - \bar{q}_s) - c_r ,$$

which can be written as

$$B_{rs}q_s - c'_r ,$$

where  $c'_r$  are the resulting constant known terms, independent of  $q_s$  at first order. After linearization, the differentiation by  $q_k$  and  $\lambda_r$  is trivial and leads to a set of linear equations

$$A_{ki}^t E_{ij}^{-1} A_{jl} q_l + B_{kr}^t \lambda_r = A_{ki}^t E_{ij}^{-1} m_j , \quad (58.4)$$

$$B_{rs} q_s = c'_r , \quad (58.5)$$

which can be expressed as

$$F_{ij}u_j = v_i , \quad (58.6)$$

where  $u_j = (q_k, \lambda_r)$  and  $v_i$  is the vector of the known constant terms running over the index  $k$  and then  $r$  in the right terms of Eq. 58.4 and Eq. 58.5, respectively. Solving the equation set in Eq. 58.6 by matrix inversion gives the the fitted quantities and their variance and covariance matrix, using the measurements and their variance and covariance matrix. The fit procedure starts by computing the linear approximation of the non-linear constraint expressions around the quantities seed values. With an iterative procedure, the unknowns are updated at each step by solving the equations and the equations are then linearized around the updated values, until the variation of the fitted unknowns is reduced below a numerically small threshold.

### References

- [1] D. Asner *et al.* (Heavy Flavor Averaging Group) (2010), [arXiv:1010.1589].
- [2] J. P. Lees *et al.* (BaBar), *Phys. Rev.* **D98**, 3, 032010 (2018), [arXiv:1806.10280].
- [3] S. Schael *et al.* (ALEPH), *Phys. Rept.* **421**, 191 (2005), [hep-ex/0506072].
- [4] J. Abdallah *et al.* (DELPHI), *Eur. Phys. J.* **C46**, 1 (2006), [hep-ex/0603044].
- [5] M. Zielinski *et al.*, *Phys. Rev. Lett.* **52**, 1195 (1984).